N-aminophthalimide as a Synthon for Heterocyclic Schiff bases: Efficient Utilization as Corrosion Inhibitors of Mild Steel in 0.5 mol.L^{-1} H$_2$SO$_4$ Solution

Mohamed M. Abdelaal[1], Saad G. Mohamed[1*], Yosry. F. Barakat[1], Hamed A. Y. Derbala[2], Hamdy H. Hassan[2] and Wail Al Zoubi[3*]

[1]Tabbin Institute for Metallurgical Studies, P.O. Box 109 Helwan 11421, Cairo, Egypt.
[2]Chemistry Department, Faculty of Science, Ain Shams University, Abbasiya, Cairo, Egypt, 11566.
[3]School of Materials Science and Engineering, Yeungnam University, Gyeongsan 38541, Republic of Korea

MANY Schiff bases were prepared to inhibit the corrosion reactions of mild steel in acidic medium. Their chemical structures were determined by using different techniques. Thermodynamic adsorption parameters of inhibitors were determined using the Langmuir adsorption isotherm. The presence of iodide ions in the medium increased the efficiency of these inhibitors. AC impedance spectroscopy was used to determine the polarization resistance. The scanning electron microscopy (SEM) showed the corrosion products decreased after using these inhibitors. The results show that the planer inhibitor is more effective than rich-electron one because it covers the whole surface. In addition, the mechanism of these inhibitors depends on decreasing the anodic and cathodic current.

Keywords: Mild steel, Inhibitor, Polarization, N-aminophthalimide, Corrosion.

Introduction

There are huge efforts to overcome the corrosion problem and many scientific papers are focused on using both phthalimides and Schiff bases as corrosion inhibitors [1-14]. Recently, phthalimide and N-phenyl derivatives were investigated to inhibit corrosion of copper and mild steel in acidic media. In addition, N-heterylphthalimides were found to be very efficient as inhibitors of mild steel in 0.5 mol.L^{-1} H$_2$SO$_4$ solution[15,16]. On the other hand, Schiff bases have potential inhibition efficiency and more than their constituent carbonyls and amines due to the presence of the imino -CH=N- functionality [17,18].

The groups, that have high electron density, have the ability to block the active centers, that causing corrosion reaction, on the metal surface by making either a chemical bond or a physical bond between those centers and inhibitors like Schiff bases and the efficiency of Schiff base inhibitors can be increased by increasing the electron. The Schiff bases, that derived from N-aminophthalimide, contain electron rich substituents that are expected to increase their inhibition action by protonation of N-atom of -CH=N- and by increasing its adsorption on the mild steel. This involves the attraction between the charged molecules and the charged metal surface favored of π-electrons of aromatic ring and ion pair of electrons on the substituents with the metal surface. Mechanism of adsorption of Schiff bases on the metal surface was mentioned in many reports [15, 19-24]. In this study, novel Schiff bases were synthesized from N-aminophthalimide and different tools investigated their structures. After that, they were used as inhibitors for mild steel in acidic solution. In addition, the adsorption mechanism and the adsorption isotherm were studied by electrochemical method. Moreover, micrographs were studied before and after adding the prepared inhibitors.

Experimental

Synthesis of inhibitors

N-aminophthalimides and their N- arylmethlene derivatives were prepared by following the literature methodologies [25-27]. All Schiff

---

bases were obtained by the condensation of a mixture of N-aminophthalimide (0.01 mol.) and different aldehydes (0.01 mol.) in ethanol.The used aldehydes were a=benzaldehyde, b=furfural, c=indole-3-aldehyde, d=piperonal, e=isatin. In the reaction of isatin, few drops of acetic acid were added to the active carbonyl group in isatin molecules. All chemicals were from Sigma-Aldrich Company. The reaction mixtures were refluxed for certain hours (monitored by TLC). Then cooled by keeping over night to obtain products, filtered, washed, and dried at 70 ºC.

Preparation of electrodes

Mild steel coupons of a surface area of 1 cm² were used as substrate after polishing with SiC emery paper up to 1200 grids and cleaning with distilled water then acetone. The chemical analysis of mild steel alloy was listed in Table 1.

Electrochemical experiments

All Electrochemical measurements(Tafel extrapolation and Electrochemical impedance spectroscopy (EIS)were carried out in 0.5 M H$_2$SO$_4$ solution without and with variant concentrations of the inhibitors at 25ºC (expect the effect of temperature)by using a Voltalab 40 Potentiostat (PGZ 301, Radiometer Analytical, France). Moreover, all electrochemical tests were carried out at its open circuit potential (it equals 30 minutes) by using a disc Pt wire and saturated calomel electrode (SCE) as an auxiliary electrode and a reference electrode, respectively. Tafel extrapolation was carried out between –700 mV and –200 mV vs. SCE. The inhibition efficiency *IE* (%) was calculated from polarization measurements by Eq.1[28]:

$$IE\ (\%) = 1 - \frac{i_{Corr(inh)}}{i_{Corr(uninh)}} \times 100 \qquad (1)$$

where $i_{Corr(uninh)}$ and $i_{Corr(inh)}$ represent the corrosion current densities for electrode without and with variant concentrations of the synthesized inhibitors, respectively.

EIS measurements were carried out in the frequency range of 100 kHz to 50 mHz with an amplitude of 10 Vat open circuit potential.*IE* (%) was determined from the polarization resistance by using Eq.2:

$$IE\ (\%) = (1 - \frac{R_{ct}^{0}}{R_{ct}}) \times 100 \qquad (2)$$

where R_{ct}^{0} and R_{ct} are the charge transfer resistances in 0.5 M H$_2$SO$_4$ solution in the uninhibited and inhibited solutions, respectively.

Results and Discussion

Identification of inhibitors

In the view of the aforementioned remarked values of inhibition efficiency of this class of organic inhibitors, this paper aims to study the concerned function of the first utilized Schiff bases S-A-E towards mild steel in 0.5 M H$_2$SO$_4$ solution. N-aryl- (S-A), N-heteryl- (S-B-D)-, and the Schiff base S-Ewere obtained by the condensation of N-aminophthalimide (S) with the corresponding aromatic aldehydes A, heterylaldehydesB-D and isatinE, respectively. This study takes into account the beneficial role that could be played by the p-electrons of the heterocyclic aldehyde or ketone N- and O- atoms present in the heterocyclic aldehyde and ketone moieties. The products' names and their symbols were listed in Table 2. The melting point, yield, time of reaction and IR spectra of products were listed in Table 3. The structure of the Schiff base S-A was confirmed by the identity of melting point and spectral data in the literature [25-27]. The infrared spectra of all the products S-A-E revealed that no coupling bonds in the 3 Mm region, signifying to the absence of the amino -NH$_2$ functionality of compound S instead a sharp absorption band appears in the region of 1604-1688 cm^{-1}characteristic to the imino -C=N- group, indicating that compound S, successfully underwent condensation reaction with the reactants carbonyl compound A-E, as shown in Figs. S1-5, (supplementary information).

Effect of inhibitor concentration

Tafel extrapolation was used to calculate the efficiency of each inhibitor. In addition, it was used to measure the effect of 1mM of iodide ions as synergism ions as well as to know the mechanism of inhibition process as shown in Fig.1-6. Tafel parameters were evaluated and recorded in Tables 4-9 where corrosion potential (E_{corr}), corrosion current density (I_{corr}), cathodic and anodic Tafel slopes (b_c and b_a) and inhibition efficiency. The analysis of data given from Tafel extrapolation shows that both cathodic and anodic currents were decreased and the shift of E_{corr} was less than 85 mV with respect to E_{corr} of the uninhibited tested solution indicated that all synthesized inhibitors are mixed type inhibitors. All tested inhibitors were decreased I_{corr} values when inhibitor doses were increased. It means that when the number of inhibitors molecules increased, they blocked the active sites in mild steel surface and decreased I_{corr}[29].From the values of corrosion current

541

N-AMINOPHTHALIMIDE AS A SYNTHON FOR HETEROCYCLIC SCHIFF BASES: EFFICIENT...

density (I_{corr}), the most effective inhibitor was S-B that had the lowest value of I_{corr}. It can be explained by the presence of a furan ring, which is considerably more reactive than benzene toward the metal surface, due to the electron-donating effect of the oxygen heteroatom that is related to the resonance into the furan ring[30]. The second effective inhibitor was inhibitor S-C then inhibitor S-D. It can be explained by the presence of pyrrole ring in the inhibitor S-C where the ion pair of nitrogen participates in the resonance of the ring and increases the electron density of the pyrrole ring, but the inhibitor S-D has four free-lone pairs of electrons at two oxygen atoms in piperonyl. After the three above inhibitors, the order of inhibition efficiency decreasing is inhibitor S-E and S-A. The ion pair of nitrogen in inhibitor S-E makes resonance with the oxygen atom at ortho position[31]. Therefore, the inhibition efficiency of this inhibitor is more than inhibitor S-A.

TABLE 1.The chemical composition of mild steel alloy.

Fe	C	Si	Mn	P	S	Cr	Ni	Al	Mo	Ti	Co
Rent	0.23	0.13	0.58	0.035	0.03	0.06	0.024	0.06	Nil	Nil	Nil

TABLE 2.The product and their symbols .
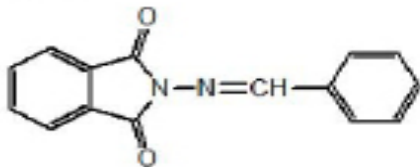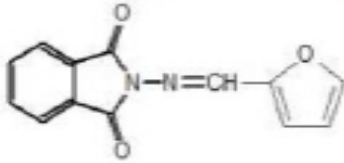
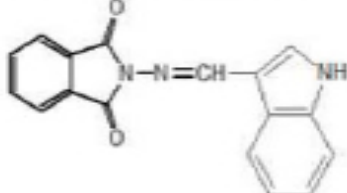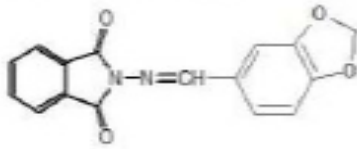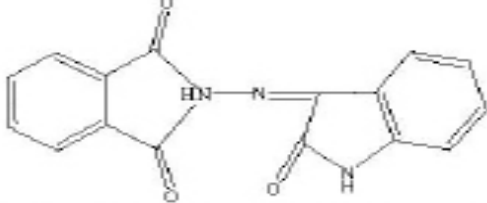| Product name	Symbol
2-(benzylideneamino)-1H-isoindole-1,3(2H)-dione	S_A
2-[(furan-2-ylmethylidene)amino]-1H-isoindole-1,3(2H)-dione	S_B
2-[(1H-indol-3-ylmethylidene)amino]-1H-isoindole-1,3(2H)-dione	S_C
2-[(1,3-benzodioxol-5-ylmethylidene)amino]-1H-isoindole-1,3(2H)-dione	S_D
2-Acetyl-benzoic acid (2-oxo-1,2-dihydro-indol-3-ylidene)-hydrazide	S_E

TABLE 3. Reaction conditions of physical data of products S_A-E.

Schiff base	Melting point (ºC)	Yield (%)	Time (min.)	IR spectra
S_A	144-147	82	90	$\upsilon_{C=O}$ 1764,1716 υ_{CN}1640
S_B	150-152	76	210	$\upsilon_{C=O}$ 1760,1723 υ_{CN}1625 υ_{NH} 3273
S_C	182-184	87	210	$\upsilon_{C=O}$ 1779,1706 υ_{CN}1623
S_D	175-177	92	120	$\upsilon_{C=O}$ 1783,1726 υ_{CN}1640 υ_{NH} 3273
S_E	258-257	93	960	$\upsilon_{C=O}$ 1785,1724 υ_{CN}1686

Fig. 1. Potentiodynamic polarization curves of mild steel electrode immersed in 0.5 M H2SO4 solution without and with different concentrations of inhibitor S in the (a) absence and (b) presence of 1mM of KI.

543

N-AMINOPHTHALIMIDE AS A SYNTHON FOR HETEROCYCLIC SCHIFF BASES: EFFICIENT...
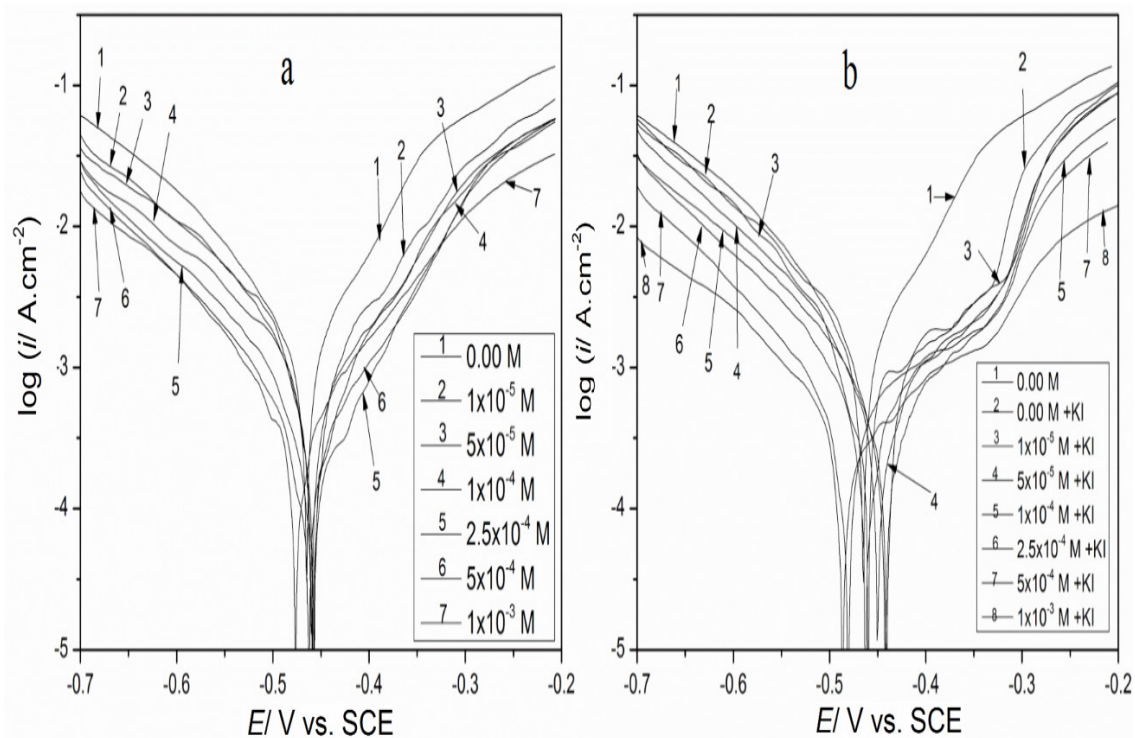
Fig. 2. Potentiodynamic polarization curves of mild steel electrode immersed in 0.5 M H2SO4 solution without and with different concentrations of inhibitor S_A in the (a) absence and (b) presence of 1mM of KI.
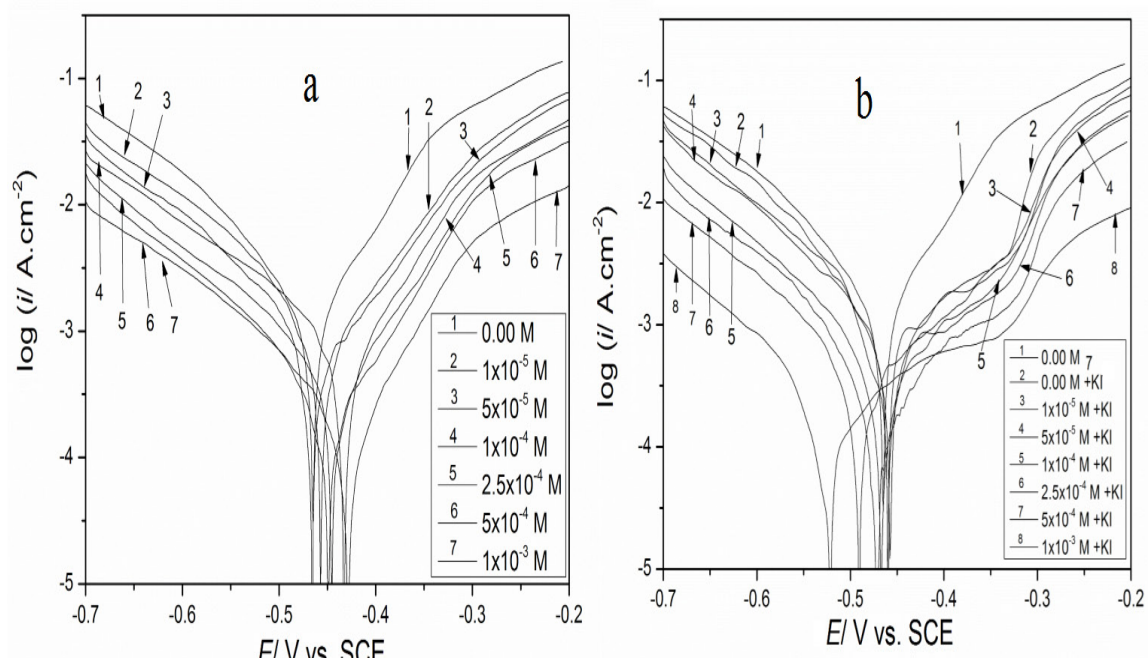
Fig. 3. Potentiodynamic polarization curves of mild steel electrode immersed in 0.5 M H2SO4 solution without and with different concentrations of inhibitor S_B in the (a) absence and (b) presence of 1mM of KI.
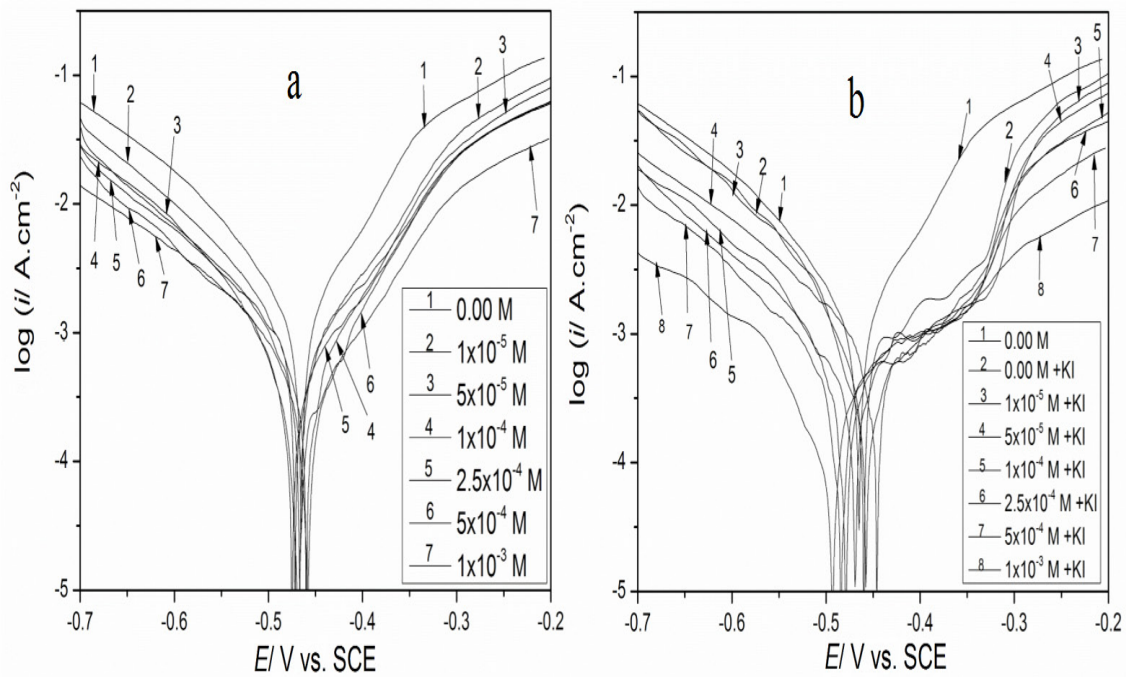
Fig.4. Potentiodynamic polarization curves of mild steel electrode immersed in 0.5 M H2SO4 solution without and with different concentrations of inhibitor S_C in the (a) absence and (b) presence of 1mM of KI.
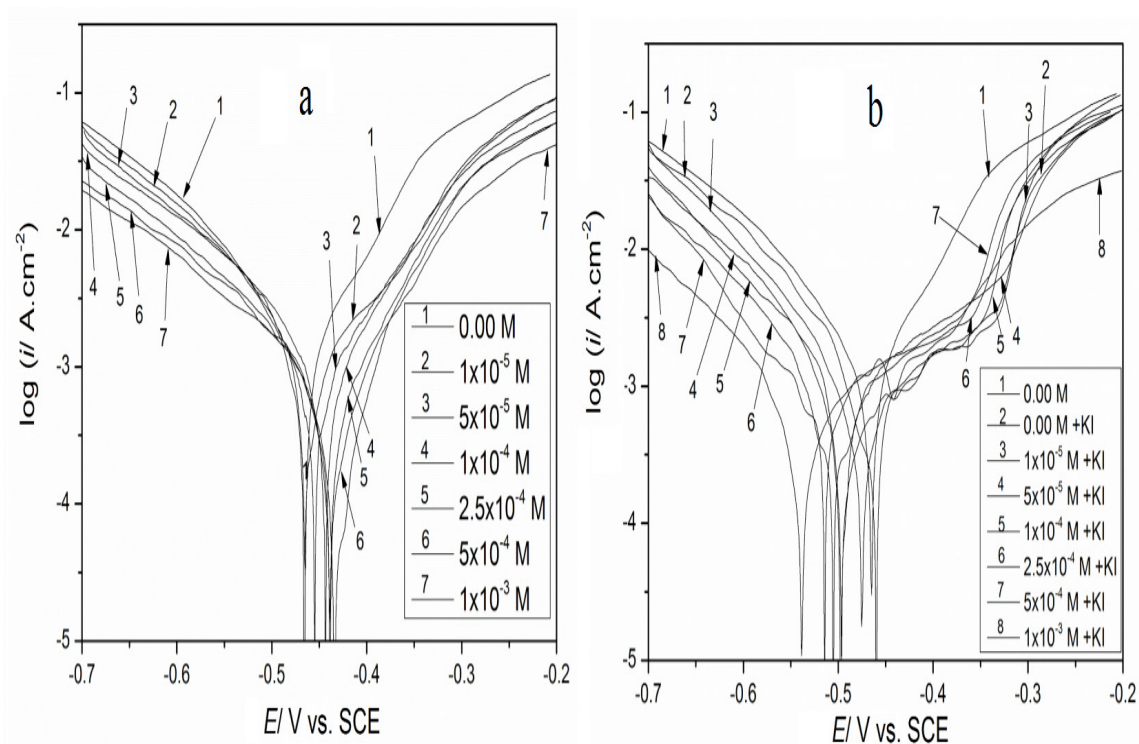

Fig. 5. Potentiodynamic polarization curves of mild steel electrode immersed in 0.5 M H2SO4 solution without and with different concentrations of inhibitor S_D in the (a) absence and (b) presence of 1mM of KI.

545

N-AMINOPHTHALIMIDE AS A SYNTHON FOR HETEROCYCLIC SCHIFF BASES: EFFICIENT...
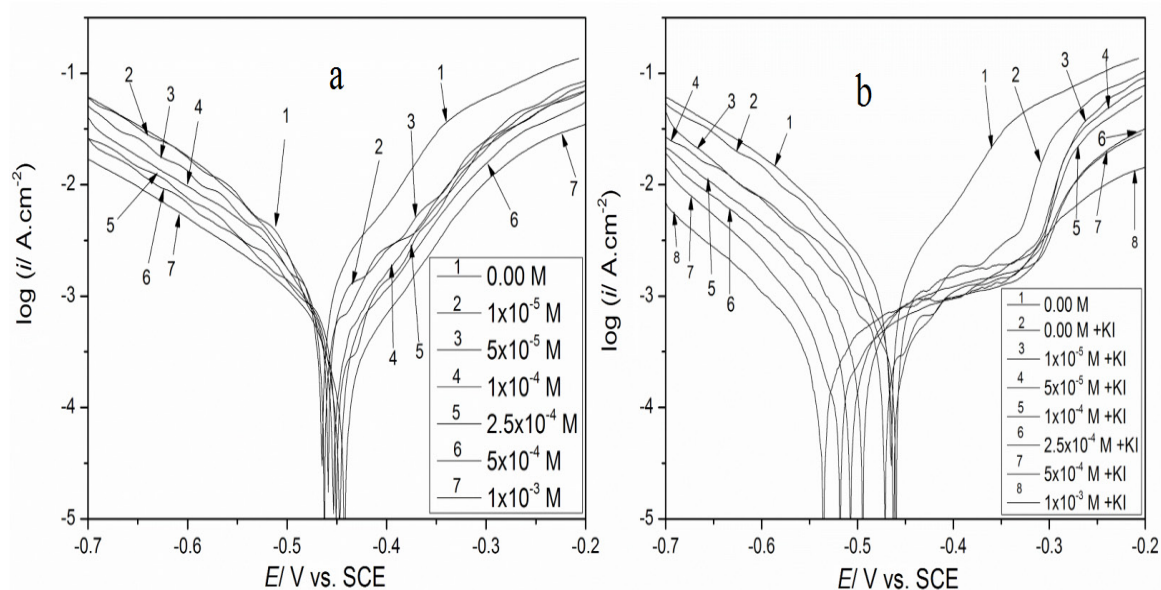
Fig. 6. Potentiodynamic polarization curves of mild steel electrode immersed in 0.5 M H2SO4 solution without and with different concentrations of inhibitor S_E in the (a) absence and (b) presence of 1mM of KI.
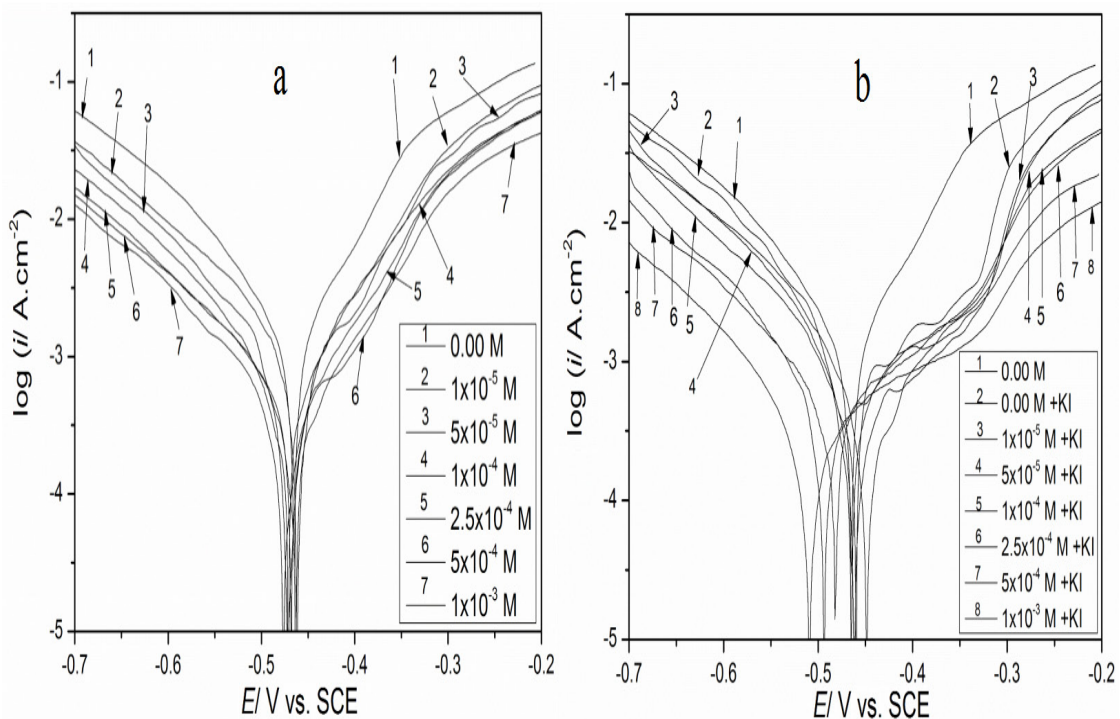
TABLE 4. Tafel parameters and IE (%) in the absence and presence of KI for inhibitor S.

Inhibitor A(M)	KI (M)	$-b_c$ (V/ dec)	b_a(V/ dec)	I_{corr}/ µA.cm^{-2}	$-E_{corr}$/Vvs. SCE	IE (%)
Blank	---------	0.112	0.097	1465	0.465	--------
Blank	1×10^{-3}	0.116	0.252	1260	0.465	13.9
1×10^{-5}	---------	0.115	0.156	1349	0.461	7.9
1×10^{-5}	1×10^{-3}	0.109	0.252	913	0.477	37.7
5×10^{-5}	---------	0.093	0.114	1193	0.461	18.6
5×10^{-5}	1×10^{-3}	0.081	0.177	848	0.494	42.1
1×10^{-4}	---------	0.134	0.098	1085	0.443	25.9
1×10^{-4}	1×10^{-3}	0.097	0.23	706	0.494	51.8
2.5×10^{-4}	---------	0.154	0.104	976	0.439	33.4
2.5×10^{-4}	1×10^{-3}	0.09	0.166	674	0.507	53.9
5×10^{-4}	---------	0.148	0.111	871	0.439	40.6
5×10^{-4}	1×10^{-3}	0.093	0.118	619	0.515	57.8
1×10^{-3}	---------	0.161	0.088	723	0.429	50.7
1×10^{-3}	1×10^{-3}	0.098	0.163	541	0.539	63.1

MOHAMED M. ABDELAAL *et al.*

TABLE 5. Tafel parameters and IE (%) in the absence and presence of KI for inhibitor S_A.

Inhibitor (M) S_A	KI (M)	$-b_c$ (V/ dec)	b_a(V/ dec)	I_{corr}/ µA.cm^{-2}	$-E_{corr}$/Vvs. SCE	IE (%)
Blank	---------	0.112	0.097	1465	0.465	--------
Blank	1 ´ 10^{-3}	0.116	0.252	1260	0.465	13.9
1 ´ 10^{-5}	---------	0.101	0.106	962	0.459	34.3
1 ´ 10^{-5}	1 ´ 10^{-3}	0.097	0.148	804	0.442	45.1
5 ´ 10^{-5}	---------	0.105	0.132	831	0.459	43.3
5 ´ 10^{-5}	1 ´ 10^{-3}	0.117	0.158	671	0.446	54.2
1 ´ 10^{-4}	---------	0.105	0.101	655	0.456	55.3
1 ´ 10^{-4}	1 ´ 10^{-3}	0.098	0.139	522	0.442	64.4
2.5 ´ 10^{-4}	---------	0.116	0.105	540	0.458	63.1
2.5 ´ 10^{-4}	1 ´ 10^{-3}	0.092	0.121	417	0.458	71.5
5 ´ 10^{-4}	---------	0.115	0.105	419	0.467	71.4
5 ´ 10^{-4}	1 ´ 10^{-3}	0.095	0.128	358	0.482	75.6
1 ´ 10^{-3}	---------	0.1	0.108	374	0.477	74.5
1 ´ 10^{-3}	1 ´ 10^{-3}	0.083	0.176	288	0.488	80.3

TABLE 6. Tafel parameters and IE (%) in the absence and presence of KI for inhibitor S_B.

Inhibitor (M) S_B	KI (M)	$-b_c$ (V/ dec)	b_a(V/ dec)	I_{corr}/ µA.cm^{-2}	$-E_{corr}$/Vvs. SCE	IE (%)
Blank	---------	0.112	0.097	1465	0.465	--------
Blank	1 ´ 10^{-3}	0.116	0.252	1260	0.465	13.9
1 ´ 10^{-5}	---------	0.084	0.098	738	0.457	49.6
1 ´ 10^{-5}	1 ´ 10^{-3}	0.107	0.152	554	0.455	62.2
5 ´ 10^{-5}	---------	0.165	0.122	576	0.464	60.7
5 ´ 10^{-5}	1 ´ 10^{-3}	0.096	0.159	432	0.458	70.5
1 ´ 10^{-4}	---------	0.089	0.084	498	0.433	66.1
1 ´ 10^{-4}	1 ´ 10^{-3}	0.103	0.165	335	0.468	77.1
2.5 ´ 10^{-4}	---------	0.101	0.092	368	0.446	74.9
2.5 ´ 10^{-4}	1 ´ 10^{-3}	0.1	0.188	234	0.472	84.1
5 ´ 10^{-4}	---------	0.119	0.093	311	0.45	78.8
5 ´ 10^{-4}	1 ´ 10^{-3}	0.079	0.131	188	0.495	87.2
1 ´ 10^{-3}	---------	0.134	0.096	250	0.429	82.9
1 ´ 10^{-3}	1 ´ 10^{-3}	0.072	0.107	107	0.524	92.7

547

N-AMINOPHTHALIMIDE AS A SYNTHON FOR HETEROCYCLIC SCHIFF BASES: EFFICIENT...

TABLE 7. Tafel parameters and IE (%) in the absence and presence of KI for inhibitor Sb_C.

Inhibitor (M) S_C	KI (M)	$-b_c$ (V/ dec)	b_a(V/ dec)	I_{corr}/ μA.cm^{-2}	$-E_{corr}$/Vvs. SCE	IE (%)
Blank	---------	0.112	0.097	1465	0.465	--------
Blank	1 ´ 10^{-3}	0.116	0.252	1260	0.465	13.9
1 ´ 10^{-5}	---------	0.108	0.101	840	0.468	42.7
1 ´ 10^{-5}	1 ´ 10^{-3}	0.091	0.23	584	0.455	60.1
5 ´ 10^{-5}	---------	0.123	0.092	683	0.457	53.4
5 ´ 10^{-5}	1 ´ 10^{-3}	0.098	0.163	511	0.449	65.1
1 ´ 10^{-4}	---------	0.096	0.101	563	0.471	61.6
1 ´ 10^{-4}	1 ´ 10^{-3}	0.093	0.105	406	0.469	72.3
2.5 ´ 10^{-4}	---------	0.088	0.098	459	0.473	68.7
2.5 ´ 10^{-4}	1 ´ 10^{-3}	0.074	0.092	313	0.477	78.6
5 ´ 10^{-4}	---------	0.079	0.091	346	0.468	76.4
5 ´ 10^{-4}	1 ´ 10^{-3}	0.063	0.074	229	0.483	84.4
1 ´ 10^{-3}	---------	0.085	0.092	313	0.458	78.6
1 ´ 10^{-3}	1 ´ 10^{-3}	0.089	0.072	163	0.495	88.9

TABLE 8. Tafel parameters and IE (%) in the absence and presence of KI for inhibitor S_D.

Inhibitor (M) S_D	KI (M)	$-b_c$ (V/ dec)	b_a(V/ dec)	I_{corr}/ μA.cm^{-2}	$-E_{corr}$/Vvs. SCE	IE (%)
Blank	---------	0.112	0.097	1465	0.465	--------
Blank	1 ´ 10^{-3}	0.116	0.252	1260	0.465	13.9
1 ´ 10^{-5}	---------	0.076	0.121	855	0.0459	41.6
1 ´ 10^{-5}	1 ´ 10^{-3}	0.102	0.167	619	0.45	57.8
5×10^{-5}	---------	0.078	0.092	727	0.461	50.4
5 ´ 10^{-5}	1 ´ 10^{-3}	0.081	0.134	530	0.465	63.8
1 ´ 10^{-4}	---------	0.098	0.101	585	0.453	60.1
1 ´ 10^{-4}	1 ´ 10^{-3}	0.086	0.165	412	0.459	71.9
2.5 ´ 10^{-4}	---------	0.083	0.089	461	0.45	68.5
2.5 ´ 10^{-4}	1 ´ 10^{-3}	0.078	0.124	335	0.485	77.1
5 ´ 10^{-4}	---------	0.077	0.08	368	0.445	74.9
5 ´ 10^{-4}	1 ´ 10^{-3}	0.069	0.122	248	0.492	83.1
1 ´ 10^{-3}	---------	0.086	0.084	277	0.442	81.1
1 ´ 10^{-3}	1 ´ 10^{-3}	0.079	0.108	176	0.507	87.9

TABLE 9. Tafel parameters and IE (%) in the absence and presence of KI for inhibitor Sb_E.

Inhibitor (M) S_E	KI (M)	$-b_c$ (V/ dec)	b_a(V/ dec)	I_{corr}/ μA.cm^{-2}	$-E_{corr}$/Vvs. SCE	IE (%)
Blank	---------	0.112	0.097	1465	0.465	--------
Blank	1 ´ 10^{-3}	0.116	0.252	1260	0.465	13.9
1 ´ 10^{-5}	---------	0.101	0.097	865	0.462	40.9
1 ´ 10^{-5}	1 ´ 10^{-3}	0.116	0.193	703	0.458	52.1
5 ´ 10^{-5}	---------	0.099	0.129	736	0.473	49.7
5 ´ 10^{-5}	1 ´ 10^{-3}	0.105	0.233	591	0.469	59.7
1 ´ 10^{-4}	---------	0.114	0.104	602	0.475	58.9
1 ´ 10^{-4}	1 ´ 10^{-3}	0.079	0.115	439	0.493	70.1
2.5 ´ 10^{-4}	---------	0.125	0.093	481	0.464	67.2
2.5 ´ 10^{-4}	1 ´ 10^{-3}	0.078	0.128	352	0.507	75.9
5 ´ 10^{-4}	---------	0.099	0.106	382	0.462	73.9
5 ´ 10^{-4}	1 ´ 10^{-3}	0.078	0.132	253	0.519	82.7
1 ´ 10^{-3}	---------	0.098	0.116	336	0.476	77.1
1 ´ 10^{-3}	1 ´ 10^{-3}	0.069	0.076	186	0.536	87.3

Synergism ion, like iodide, is used to improve the inhibition efficiency and to minimize the amount of inhibitor in the inhibitive system [32]. The interaction between iodide ions and the surface is stronger than inhibitors; therefore, there is anodic breakdown potential that reflects the presence of anodic protective film on the mild steel surface as shown in Figs. (1b, 2b, 3b,4b, 5b and 6b). The adsorbed iodide ions attract the inhibitor from the bulk solution to adsorb on it and decrease the current density[32]. For example, As shown in Table 6, when 1 mM KI was added into the 0.5 M H$_2$SO$_4$solution containing 1 mM of Inhibitor (S-B), the current density reduced from 250 μA/cm^2 to 107 μA/cm^2. Moreover, the values of E_{corr}were shifted to more negative (cathodic) direction due to blocking the active sites on the surface after adding inhibitor dose[33]. Adding 1 mM of iodide ions with inhibitor dose as synergism ions increased the corrosion protection because the iodide ion has a negative charge that attracts the inhibitor cation and the positively charged metal surface, as well, and iodide ions act as a bridge[34]. The synergistic effect could be calculated by the surface coverage (θ) by using Eq.3[35].

$$\theta = \frac{i_{Corr(uninh)} - i_{Corr(inh)}}{i_{Corr(uninh)}} \quad (3)$$

where $i_{Corr(uninh)}$and $i_{Corr(inh)}$ are described above. Aramaki and Hackerman [36] calculated the synergism parameterS_θ using by Eq.4

$$S_\theta = \frac{1 - \theta_{1+2}}{1 - \theta'_{1+2}} \quad (4)$$

where $\theta_{1+2} = (\theta_1 + \theta_2) - (\theta_1\theta_2)$, θ_1 is the surface coverage by 1 mM of KI, θ_2 is the surface coverage by the inhibitor,θ'_{1+2} is the measured surface coverage by both.

The values of $S_\theta$can be used to gain more information about the relation between the synergism ions and the inhibitor molecules on the surface if it is co-operative or competitive [37]. The charge on the iodide ions is negative and the values of S_θ are higher than unity, as shown in Table 10, which is mean, that iodide ions adsorbed on the surface, which carried positive charges, to form intermediate bridges between the surface and the inhibitor cations, as well.

549

N-AMINOPHTHALIMIDE AS A SYNTHON FOR HETEROCYCLIC SCHIFF BASES: EFFICIENT...

TABLE 10. The synergism parameter S$_\theta$ for each inhibitor.

Concn.(M)	Synergism parameter (S$_\theta$)					
	S	S_A	S_B	S_C	S_D	S_E
1×10^{-5}	1.27	1.03	1.15	1.24	1.19	1.06
5×10^{-5}	1.21	1.1	1.15	1.15	1.18	1.07
1×10^{-4}	1.32	1.1	1.28	1.19	1.22	1.18
2.5×10^{-4}	1.24	1.14	1.35	1.26	1.18	1.18
5×10^{-4}	1.21	1.04	1.43	1.44	1.28	1.3
1×10^{-3}	1.15	1.1	2.02	1.66	1.56	1.55

Electrochemical impedance spectroscopy (EIS)

Corrosion resistance, that increases after addition of the inhibitor, could be measured by EIS due to the formation of a layer of inhibitor molecules on the surface which decreases the corrosion rate [38, 39]. In this work, the corrosion behavior of tested samples, in the blank solution and in the presence of 1 mM of each inhibitor, was studied by EIS. Fig.7a represents Nyquist plots that draw a semicircle and its diameter expands with the increasing of inhibitor efficiency. The semicircle consists of a depressed capacitive loop and a small inductive loop at high frequency (HF) and low frequency (LF), respectively. R_{ct} is the charge transfer resistance and its value is the difference between the high-frequency impedance and the low-frequency one as shown in Eq.5[40]:

$$R_{ct} = Z_{re} \text{ (at low frequency)} - Z_{re} \text{ (at high frequency)} \quad (5)$$

where Z_{re} represents the real element of the impedance. In general, the constant phase element (*CPE*) uses instead of the pure double layer capacitor as a result of the surface roughness to give a more accurate fit in the equivalent circuit [41]. The correct value of double layer capacitance C_{dl} was determined at the frequency f_{max}, at which the imaginary element of the impedance is, by Eq.6[40]:

$$C_{dl} = P (\omega_{max})^{n-1} \quad (6)$$

where P is the magnitude of the CPE, $\omega_{max} = 2\pi f_{max}$; f_{max} represents the frequency at maximum value of imaginary resistance and n value is a factor that satisfies the condition $0 \leq n \leq 1$, which n = 1 in an ideal capacitor and n < 1 in CPE. The parameters n and C_{dl} are independent of frequency. *Rs* is the ohmic resistance between the working and the reference electrode; CPE is the capacitance of the electrical double-layer

in the system; L is the inductor related to the relaxation process obtained from adsorption species. The EIS data fitting by equivalent circuit was listed in Table 11. It is clear that R_s values increased with all inhibitors, it refers to decrease the conductivity of the solution. The R_{ct} values increased when tested inhibitors were added to the system, indicating that those inhibitors adsorbed on the surface and form a protective film between the solution and the surface[42]. Both EIS results and Tafel results confirmed the inhibition efficiencies of the tested inhibitors minimizes in the order: S-B > S-C > S-E > S-D>S-A > S. The electron density on the inhibitor molecules caused a decrease in the C_{dl} values, which means the thickness of the double layer in the solution expands. These results indicate that these inhibitors adsorbed on the mild steel/solution interface[43,44]. It is easy to observe that there is an increase in the R_{CPE} values with decreasing of n value when compared to that obtained in pure 0.5 M H_2SO_4 solution. It may be related to a decrease in the surface heterogeneity resulting from the interaction between any inhibitor and the active centers [45]. The presence of inductive R_L-$L1$ loop at *LF* may be related to either the relaxation process and its dielectric properties obtained from SO_4^{-2} and H_{ads}^+ which adsorb on the mild steel surface[46] or the decomposition of the passivated surface at low frequencies[47].

Fig.7b shows that Bode plots divide into three parts. The first one represents the solution resistance where the log |Z| values at HF tend to become zero and the phase angle shifts to 0°. The second part, in the medium frequency region where the slope of the relation between log |Z| and log frequency is near to -1 and the phase angle equals about -90°. This response represents a

capacitive behavior but not an ideal capacitor that has the slope equals -1 and the phase angle equals -90°. Therefore, the ideal capacitor was replaced by *CPE*. The last part at low frequency where the resistance of the mild steel electrode increases but the log |*Z*| values do not depend on the frequency, i.e. the major current at this region was dc and the minor was ac [48].

Effect of temperature and activation parameters of inhibition process

For many metals and alloys, such as mild steel, the temperature of the medium directly affects the corrosion rate like any chemical reactions. The elevating of temperature leads to increase the rate of diffusion of oxygen, which is an important factor in the corrosion process. However, the corrosion rate decreases at the boiling point because of the solubility of oxygen decreases[49]. As shown in Table 12, the current density increased with increasing temperature from 298-348 kelvin in the blank solution and in the inhibited solution by 1 mM of inhibitor, (Figs. S6-12, supplementary information). It refers to an increase in desorption of those inhibitors followed by dissolution of the surface. The current density of mild steel also increased exponentially in acidic medium with increasing the temperature due to decreasing of hydrogen evolution overpotential [50]. In order to gain more information about the corrosion process, the activation energy and thermodynamic parameters were determined by Arrhenius Eq.7and transition state Eq.8[51]:

$$r = \lambda \exp\left(-\frac{E_a}{RT}\right) \qquad (7)$$

$$r = \frac{RT}{Nh} \exp\left(\frac{\Delta S^*}{R}\right) \exp\left(-\frac{\Delta H^*}{RT}\right) \qquad (8)$$

where λ represents the Arrhenius pre-exponential factor. R represents the universal gas constant and T represents the absolute temperature. E_a represents the activation corrosion energy, h represents the Planck's constant, N represents the Avogadro's number and r is the rate of metal dissolution reaction, which is directly related to corrosion current density (I_{corr}). ΔS^* represents the entropy of activation, ΔH^* represents the enthalpy of activation, at 1 mM of inhibitors, are calculated by linear regression between ln (I_{corr}) and 1/ *T*as shown in Fig.8. All the linear regression coefficients are close to 1, refers that the mild steel corrosion in this system can be explained using the

kinetic model. Fig.9 shows a plot of ln (I_{corr}/T) versus (1/ *T*). Straight lines were obtained with a slope of (-$\Delta H^*/R$) and an intercept of ((ln (*R/Nh*)) +($\Delta S^*/R$)) from which the values of $\Delta H^*$and ΔS^*weredetermined and listed in Table 13. From the data obtained, E_a values increased after inhibitors addition, indicating a strong adsorption of those inhibitors [52]. The increasing of positive values of ΔH^* means that the dissolution reaction of mild steel after inhibitors addition became more difficult due to increase the height of energy barrier of this reaction. The large values and minus signs of $\Delta S^*$for the inhibited and uninhibited systems refer to the activation complex preferred to the association rather than dissolution direction [53]. This behavior of Schiff base inhibitors at elevated temperatures in acidic medium is in good agreement with other studies [54-56]

The adsorption isotherm

The mechanism of Schiff bases electrochemical reaction can be determined by adsorption isotherms. The plot of *C/Θ* versus *C* gave a straight line as shown in Fig.10. It means that the adsorption of studied inhibitors in 0.5 M H_2SO_4 solution follows the Langmuir's adsorption isotherm, Eq.9, for the five investigated compounds [57].

$$\frac{C}{\theta} = \frac{1}{K_{ads}} + C \qquad (9)$$

where C is the inhibitor concentration in the bulk of the solution, θ is the surface coverage (θ = *IE*/100) and K_{ads} is the adsorption-desorption equilibrium constant which is related to the standard free energy adsorption,ΔG^o_{ads} at a single temperature can be calculated from Eq.10[58]:

$$\Delta G^o_{ads} = -RT \ln(55.5 K_{ads}) \qquad (10)$$

where 55.5 is the molar concentration of water, R is the universal gas constant, and T is the temperature in Kelvin. The values of linear regression coefficients (R^2), K_{ads} and ΔG^o_{ads} were listed in Table 14. The type of adsorption of these inhibitors could be determined from the values of ΔG^o_{ads}[59]. All ΔG^o_{ads}values of those inhibitors are less than -20 KJ/mol., which mean they obey physisorption mechanism and the strength order of them as following: S-B > S-C > S-E > S-D > S-A > S.

551

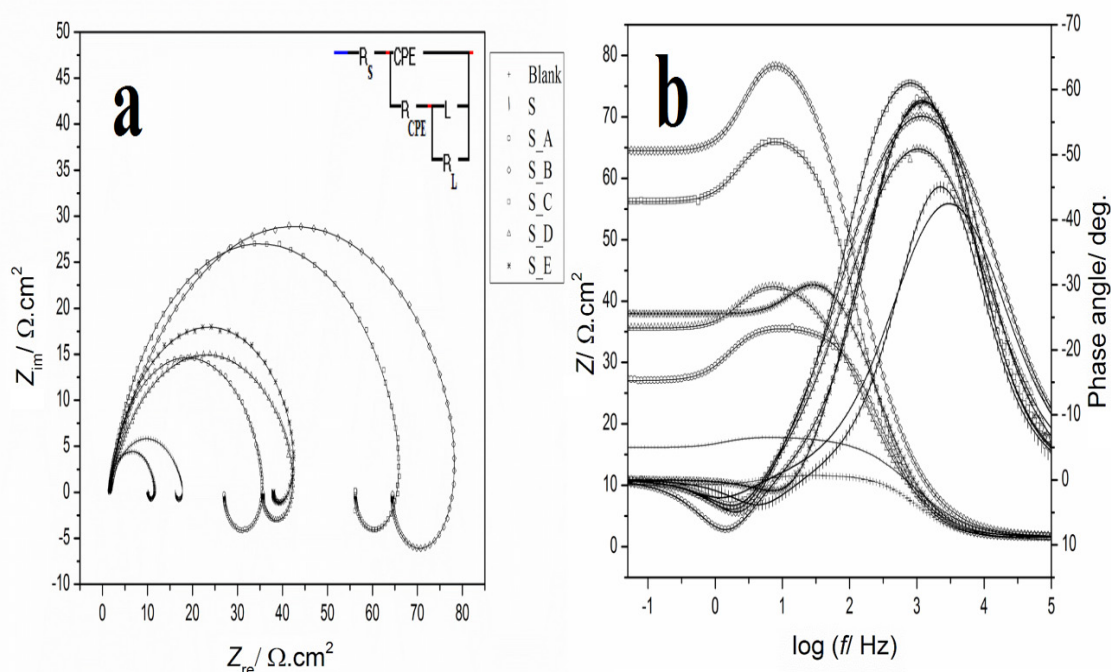N-AMINOPHTHALIMIDE AS A SYNTHON FOR HETEROCYCLIC SCHIFF BASES: EFFICIENT...

Fig. 7. (a) Nyquist plots and the equivalent circuit model (inset) used for fitting the impedance spectra and (b) Bode plots of mild steel in the uninhibited and inhibited 0.5 M H2SO4 solutions containing 1 mM of each inhibitor.

TABLE 11. Results of EIS data fitting by the equivalent circuit.

	$R_S/$ $(\Omega.cm^2)$	$R_{CPE}/$ $(\Omega.cm^2)$	$R_L/$ $(\Omega.cm^2)$	$P/$ $(\mu F.cm^{-2})$	n	L/H	$C_{dl}/$ $(\mu F.cm^{-2})$	$R_{ct}/$ $(\Omega.cm2)$	$IE\%$
Blank	1.44	8.66	1.62	4.75E-05	0.94	0.05	28.33	9.67	…
S	1.50	14.673	1.8458	9.58E-05	0.8138	0.21099	21.39	16.26	40.53
S_A	1.51	25.53	9.04	4.84E-05	0.88	0.81	19.57	34.01	71.57
S_B	1.61	62.9	19.68	7.87E-05	0.73	0.99	14.17	76.49	87.36
S_C	1.68	54.52	12.32	5.04E-05	0.83	0.77	16.55	64.91	85.10
S_D	1.58	36.38	8.1	4.54E-05	0.87	0.08	17.98	40.74	76.26
S_E	1.51	34.13	9.23	1.34E-04	0.72	0.56	18.12	39.76	75.68

TABLE 12. The relation between IE (%) of each inhibitor and the temperature.

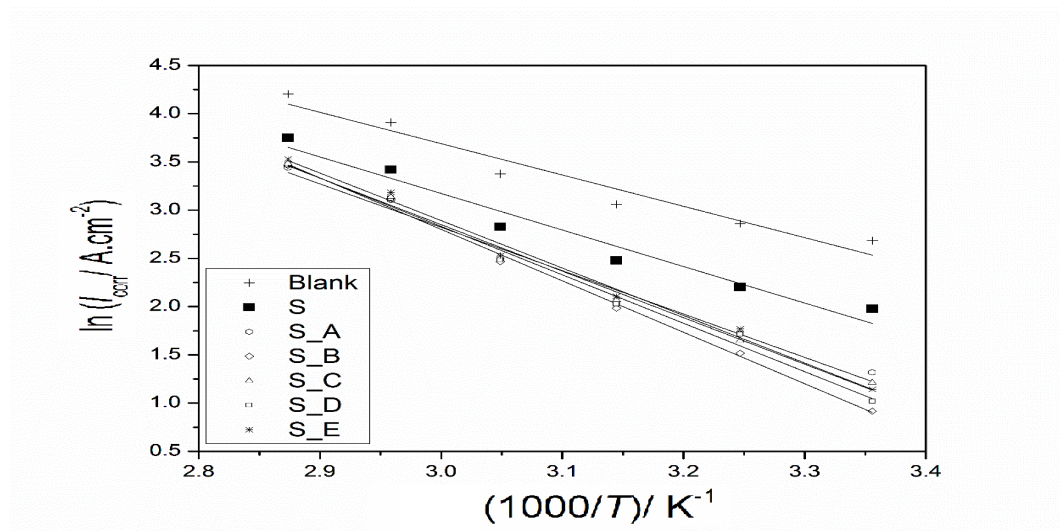| Temperature (K)	IE (%)					
	S	S_A	S_B	S_C	S_D	S_E
298	50.7	74.5	82.9	81.1	77.6	78.1
308	48.3	68.1	73.9	70.4	68.2	66.5
318	44.1	64.2	65.9	62.9	64.6	61.4
328	42.2	58.7	59.8	57.4	58.9	57.2
338	38.6	55.2	55.1	53.7	54.4	51.6
348	36.4	53.4	52.2	51.2	52.1	48.9

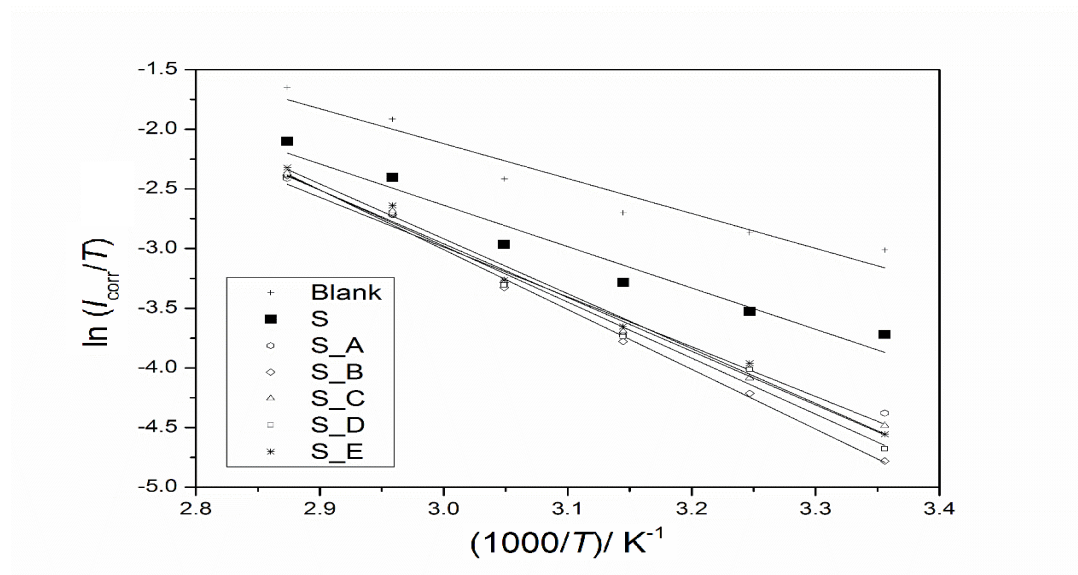**Fig. 8. Arrhenius plots of ln Icorr versus 1/T for mild steel in 0.5 M H2SO4 solution.**

Fig. 9. Plots of ln Icorr/T versus 1/T for mild steel in 0.5 M H2SO4 solution.

TABLE 13. E_a, ΔH^* and ΔS^* of the dissolution of carbon steel in 0.5 M H_2SO_4 in the absence and presence of 1 mM of the investigated inhibitors.

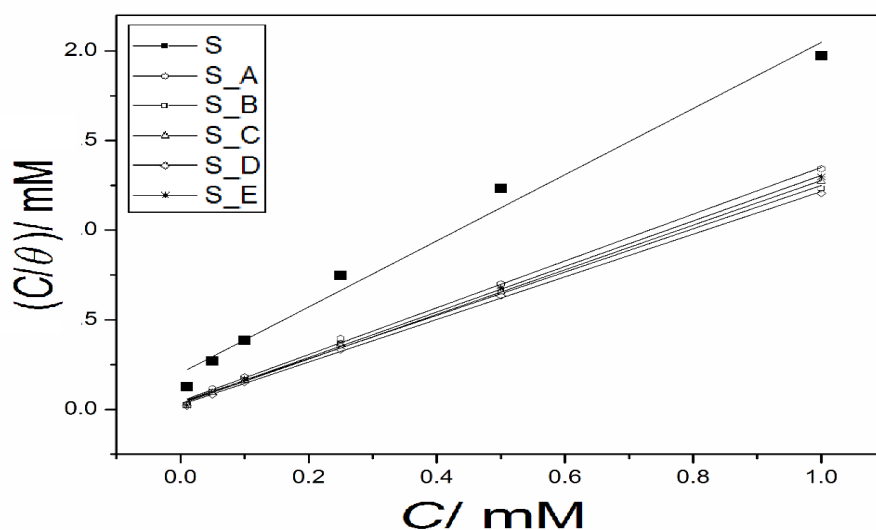| Inhibitor	E_a (KJ / mol.)	ΔH^* (KJ / mol.)	ΔS^*(J /k mol.)
Blank	26.9	24.2	-142.2
S	31.4	28.7	-132.8
S_A	37.3	34.6	-118.1
S_B	44.3	41.6	-97.4
S_C	40.9	38.3	-107.1
S_D	40.2	37.5	-109.3
S_E	39.2	36.6	-111.7

Fig. 10. The Langmuir adsorption isotherm plots for the adsorption of inhibitors in 0.5 M H2SO4 on the surface of mild steel.

TABLE 14. The values of linear regression coefficients (R^2), K_{ads} and ΔG^o_{ads} ΔG^o_{ads} .

Inhibitors	R^2	K_{ads} (M⁻¹)	ΔG^o_{ads} ΔG^o_{ads} (KJ/mol.)
S	0.986	4.95	-13.890047
S_A	0.998	22.22	-17.60
S_B	0.999	38.46	-18.96
S_C	0.998	24.39	-17.84
S_D	0.999	29.41	-18.29
S_E	0.999	27.78	-18.16

The scanning electron micrographs (SEM) observation

For morphological observations of mild steel specimens and inhibition actions of the inhibitors, SEM photography was taken before and after immersion in the blank solution for 24 h in the absence and presence of 1 mM of all inhibitors that prepared in this study and inhibitor S as well, as shown in Figs.11 and 12a-e. It can be seen in SEM images the reactions products covered the surface of the sample in uninhibited solution(Fig. 12b) that consist of iron oxides and ferrous sulfate layer [11]. Inhibitor S decreased the corrosion products on the surface, however,

they could be observed in Fig. 12a. It means that the protective film of inhibitor S was weak. The corrosion products decreased significantly with other inhibitors because the inhibitors made a strong film on the surface, as shown in Fig. 12b-h. There were no corrosion products in the presence of inhibitors S-B and S-C due to high inhibition efficiency of them, as observed in Fig. 12c and Fig. 12d. These images confirmed the electrochemical test results that obtained before.
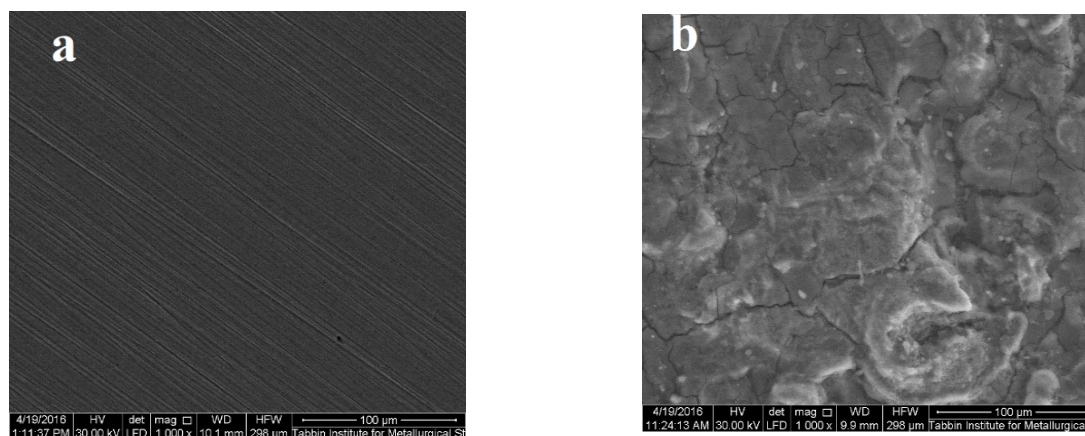
MOHAMED M. ABDELAAL *et al.*

Fig. 11. SEM images of mild steel (a) before and (b) after immersion in 0.5 mol.L-1 H2SO4for 24 h.
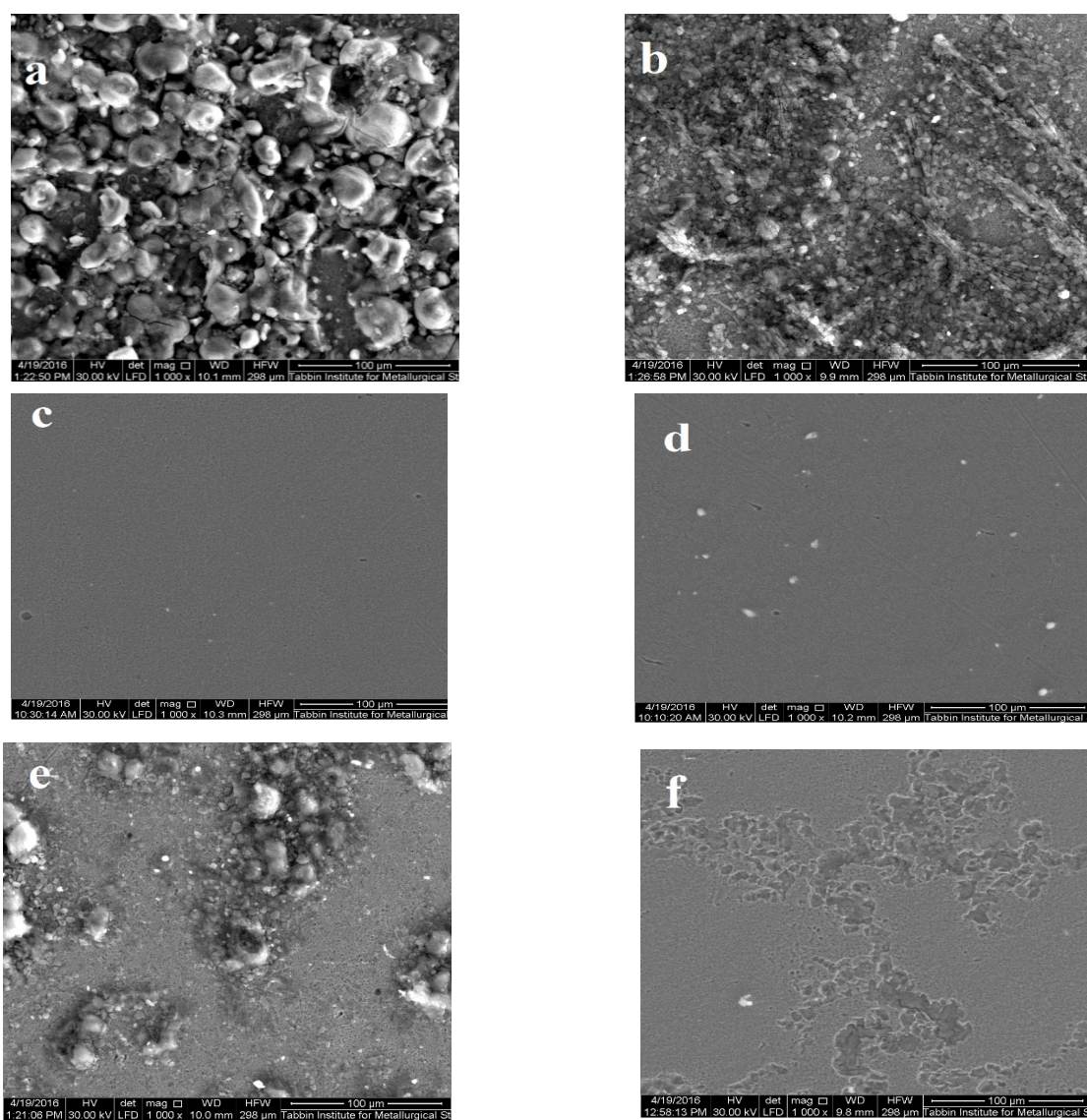

Fig. 12. SEM images of mild steel after immersion in 0.5 mol.L-1 H2SO4 for 24 h in presence of 1 mM of inhibitor (a) S, (b) S_A, (c) S_B, (d) S_C, (e) S_D, (f) S_E.

555

N-AMINOPHTHALIMIDE AS A SYNTHON FOR HETEROCYCLIC SCHIFF BASES: EFFICIENT...

Conclusions

Many Schiff bases have been prepared from n-aminophthalimide and different aldehydes. The melting point and IR were investigated the imino -C=N- group on them. They were used as corrosion inhibitors for mild steel in acidic medium and increased the protection from corrosion with an increasing in inhibitors dose. Addition of iodide ions to the system formed a protective layer and raised the inhibition efficiency of those inhibitors. Tafel plots proved that these inhibitors are mixed-type inhibitors. The inhibition efficiency of these Schiff bases decreased with an increasing in temperature. EIS data showed that the inhibitors increased the corrosion resistance as shown in SEM images and increased the double layer capacitance due to adsorption of them on the surface and blocked the active sites. The inductive loop in Nyquist diagrams was related to the relaxation process by adsorption species. The adsorbed inhibitor molecules on the surface follow Langmuir adsorption isotherm model. The standard free energy proved that the adsorption of those inhibitors on mild steel is spontaneously physisorption.

References

1. Ashassi-Sorkhabi H., Shaabani B., Seifzadeh D., Corrosion inhibition of mild steel by some schiff base compounds in hydrochloric acid. *Applied Surface Science* **239**, 154-164 (2005).

2. Emregül K.C., Atakol O., Corrosion inhibition of iron in 1M HCl solution with Schiff base compounds and derivatives. *Materials Chemistry and Physics* **83**, 373-379 (2004).

3. Hamak K.F., Synthetic of Phthalimides via the reaction of phthalic anhydride with amines and evaluating of its biological and anti corrosion activity. *International Journal of Chem Tech Research* **6**, 324-333 (2014).

4. Hegazy M.A., A novel Schiff base-based cationic gemini surfactants: Synthesis and effect on corrosion inhibition of carbon steel in hydrochloric acid solution. *Corrosion Science* **51**, 2610-2618 (2009).

5. Hosseini M., Mertens S.F.L., Ghorbani M., Arshadi M.R., Asymmetrical Schiff bases as inhibitors of mild steel corrosion in sulphuric acid media. *Materials Chemistry and Physics* **78**, 800-808 (2003).

6. Keles H., Keles M., Dehri I., Serindag O., Adsorption and inhibitive properties of aminobiphenyl and its Schiff base on mild steel corrosion in 0.5 M HCl medium. *Colloids and Surfaces A: Physicochemical and Engineering Aspects* **320**, 138-145 (2008).

7. Yurt A., Duran B., Dal H., An experimental and theoretical investigation on adsorption properties of some diphenolic Schiff bases as corrosion inhibitors at acidic solution/mild steel interface. *Arabian Journal of Chemistry* **7**,732-740 (2014).

8. Emregül K.C., Kurtaran R., Atakol O., An investigation of chloride-substituted Schiff bases as corrosion inhibitors for steel. *Corrosion Science* **45**, 2803-2817 (2003).

9. Da Silva A.B., D'Elia E., Da Cunha Ponciano Gomes J.A., Carbon steel corrosion inhibition in hydrochloric acid solution using a reduced Schiff base of ethylenediamine. *Corrosion Science* **52**, 788-793 (2010).

10. Negm N.A., Elkholy Y.M., Zahran M.K., Tawfik S.M., Corrosion inhibition efficiency and surface activity of benzothiazol-3-ium cationic Schiff base derivatives in hydrochloric acid. *Corrosion Science* **52**, 3523-3536 (2010).

11. Hasanov R., Sadikoglu M., Bilgiç S., Electrochemical and quantum chemical studies of some Schiff bases on the corrosion of steel in H_2SO_4 solution. *Applied Surface Science* **253**, 3913-3921 (2007).

12. Desai M.N., Desai M.B., Shah C.B., Desai S.M., Schiff bases as corrosion inhibitors for mild steel in hydrochloric acid solutions. *Corrosion Science* **26**, 827-837 (1986).

13. Shokry H., Yuasa M., Sekine I., Issa R.M., El-baradie H.Y., Gomma G.K., Corrosion inhibition of mild steel by schiff base compounds in various aqueous solutions: part 1. *Corrosion Science* **40**, 2173-2186 (1998).

14. Makhlouf M.T., Gomma G.K., Wahdan M.H., Khalil Z.H., Effect of cyanine dye-solvent interaction on the electrochemical corrosion behaviour of low-carbon steel in acid medium. *Materials Chemistry and Physics* **40**,119-125 (1995).

15. Chitra S., Parameswari K., Selvaraj A., Dianiline schiff bases as inhibitors of mild steel corrosion in acid media. *International Journal of Electrochemical Science* **5**,1675-1697 (2010).

16. Sethi T., Chaturvedi A., Upadhyay R., Mathur S., Corrosion inhibitory effects of some Schiff's bases on mild steel in acid media. *Journal of the Chilean Chemical Society* **52**, 1206-1213 (2007).

17. Şafak S., Duran B., Yurt A., Türkoğlu G., Schiff bases as corrosion inhibitor for aluminium in HCl solution. *Corrosion Science* **54**, 251-259 (2012).

18. Ghasemi O., Ghadimi M.R., Ghasemi V., Adsorption and Inhibition Effect of Benzaldehyde Schiff Bases on Mild Steel Corrosion in 1 M HCl Medium. *Journal of Dispersion Science and Technology* **35**,1143-1154 (2014).

19. Bentiss F., Traisnel M., Lagrenee M., Influence of 2,5-bis(4-dimethylaminophenyl)-1,3,4-thiadiazole on corrosion inhibition of mild steel in acidic media. *Journal of Applied Electrochemistry* **31**, 41-48 (2001).

20. Aytaç A., Özmen U., Kabasakaloglu M., Investigation of some Schiff bases as acidic corrosion of alloy AA3102. *Materials Chemistry and Physics* **89**, 176-181 (2005).

21. Gomma G.K., Wahdan M.H., Schiff bases as corrosion inhibitors for aluminium in hydrochloric acid solution. *Materials Chemistry and Physics* **39**, 209-213 (1995).

22. Yurt A., Ulutas S., Dal H., Electrochemical and theoretical investigation on the corrosion of aluminium in acidic solution containing some Schiff bases. *Applied Surface Science* **253**, 919-925 (2006).

23. Issa R.M., Awad M.K., Atlam F.M.D.F.T., theoretical studies of antipyrine Schiff bases as corrosion inhibitors. *Materials and Corrosion* **61**, 709-714 (2010).

24. Safak S., Duran B., Yurt A., Turkoglu G., Schiff bases as corrosion inhibitor for aluminium in HCl solution. *Corrosion Science.* **54**, 251-259 (2012).

25. Lee G.E., Heffner R.J., Method for synthesizing N-aminophthalimide, U.S. *Patent No* **4**, 720, 553 (1988).

26. Derbala H., Synthesis and Some Reactions of 3, 4-Dimethoxyphenylmethyleneaminophthalimide. ChemInform 25 (1994).

27. Derbala H.A., Chemoselectivity of 2-Arylmethyleneaminoisoindolin-1, 3-diones toward Arenes under Friedel–Crafts Conditions: An Efficient Synthesis of Benzophenones Integrated with 2-Substituted Hydrazone Moieties.

Egypt.J.Chem. **61**, No.3 (2018)

28. Saliyan V.R., Adhikari A.V., Quinolin-5-ylmethylene-3-{[8-(trifluoromethyl)quinolin-4-yl]thio}propanohydrazide as an effective inhibitor of mild steel corrosion in HCl solution. *Corrosion Science* **50**,55-61 (2008).

29. Fouda A..S, Ellithy A.S., Inhibition effect of 4-phenylthiazole derivatives on corrosion of 304L stainless steel in HCl solution. *Corrosion Science* **51**, 868-875 (2009).

30. Abraham R., Bernstein H., The proton resonance spectra of furan and pyrrole. *Canadian Journal of Chemistry* **37**, 1056-1065 (1959).

31. Davidovich P., Novikova D., Tribulovich V., Smirnov S., Gurzhiy V., Melino G., Garabadzhiu A., First X-ray structural characterization of isatin Schiff base derivative. NMR and theoretical conformational studies. *Journal of Molecular Structure* **1075**, 450-455 (2014).

32. Li X., Deng S., Fu H., Synergism between red tetrazolium and uracil on the corrosion of cold rolled steel in H_2SO_4 solution. *Corrosion Science* **51**,1344-1355 (2009).

33. Cao C., On electrochemical techniques for interface inhibitor research. *Corrosion Science.* **38**, 2073 (1996).

34. Umoren S., Ebenso E., The synergistic effect of polyacrylamide and iodide ions on the corrosion inhibition of mild steel in H 2 SO 4. *Materials Chemistry and Physics* **106**, 387-393 (2007).

35. Behpour M., Ghoreishi S.M., Soltani N., Salavati-Niasari M., The inhibitive effect of some bis-N,S-bidentate Schiff bases on corrosion behaviour of 304 stainless steel in hydrochloric acid solution. *Corrosion Science* **51**,1073-1082 (2009).

36. Aramaki K., Hackerman N., Inhibition Mechanism of Medium-Sized Polymethyleneimine. *Journal of The Electrochemical Society* 116 (1969).

37. Umoren S., Ogbobe O., Igwe I., Ebenso E., Inhibition of mild steel corrosion in acidic medium using synthetic and naturally occurring polymers and synergistic halide additives. *Corrosion Science* **50**,1998-2006 (2008).

38. Fonatana M.G., Greene N.D., *Corrosion Engineering,* McGraw-Hill, New York (1978).

39. Bard A.J., Faulkner L.R., *Electrochemical*

557

N-AMINOPHTHALIMIDE AS A SYNTHON FOR HETEROCYCLIC SCHIFF BASES: EFFICIENT...

methods : fundamentals and applications, Wiley, New York (2001).

40. Hsu C.H., Mansfeld F., Technical Note: Concerning the Conversion of the Constant Phase Element Parameter Y0 into a Capacitance. *Corrosion* **57**,747-748 (2001).

41. Benedeti A., Sumodjo P., Nobe K., Cabot P., Proud W., Electrochemical studies of copper, copper-aluminium and copper-aluminium-silver alloys: Impedance results in 0.5 M NaCl. *Electrochimica Acta* **40**, 2657-2668 (1995).

42. Bentiss F., Traisnel M., Lagrenee M., The substituted 1,3,4-oxadiazoles: a new class of corrosion inhibitors of mild steel in acidic media. *Corrosion Science* **42**,127-146 (2000).

43. Rehim S.S.A., Hazzazi O.A., Amin M.A., Khaled K.F., On the corrosion inhibition of low carbon steel in concentrated sulphuric acid solutions. Part I: Chemical and electrochemical (AC and DC) studies. *Corrosion Science* **50**, 2258-2271 (2008).

44. Ashassi-Sorkhabi H., Seifzadeh D., Hosseini M., E.N, EIS and polarization studies to evaluate the inhibition effect of 3H-phenothiazin-3-one, 7-dimethylamin on mild steel corrosion in 1M HCl solution. *Corrosion Science* **50**, 3363-3370 (2008).

45. Benali O., Larabi L., Mekelleche S., Harek Y., Influence of substitution of phenyl group by naphthyl in a diphenylthiourea molecule on corrosion inhibition of cold-rolled steel in 0.5 M H$_2$SO$_4$. *Journal of Materials Science* **41**,7064-7073 (2006).

46. Lenderink H., Linden M., De Wit J., Corrosion of aluminium in acidic and neutral solutions. *Electrochimica acta* **38**, 1989-1992 (1993).

47. Sherif E., Park S-M., Effects of 1, 4-naphthoquinone on aluminum corrosion in 0.50 M sodium chloride solutions. *Electrochimica Acta* **51**,1313-1321 (2006).

48. Mansfeld F., Kendig M., Tsai S., Recording and analysis of AC impedance data for corrosion studies. *Corrosion* **38**, 570-580 (1982).

49. Gerasimov V.V., Rozenfeld I.L., Effect of temperature on the rate of corrosion of metals. *Bulletin of the Academy of Sciences of the USSR, Division of Chemical Science* **6**,1192-1197 (1957).

50. Popova A., Sokolova E., Raicheva S., Christov M., AC and DC study of the temperature effect on mild steel corrosion in acid media in the presence of benzimidazole derivatives. *Corrosion Science* **45**, 33-58 (2003).

51. Achary G., Sachin H.P., Naik Y.A., Venkatesha T.V., The corrosion inhibition of mild steel by 3-formyl-8-hydroxy quinoline in hydrochloric acid medium. *Materials Chemistry and Physics* **107**, 44-50 (2008).

52. Morad M., Inhibition of iron corrosion in acid solutions by Cefatrexyl: Behaviour near and at the corrosion potential. *Corrosion Science* **50**, 436-448 (2008).

53. Noor E.A., Al-Moubaraki A.H., Thermodynamic study of metal corrosion and inhibitor adsorption processes in mild steel/1-methyl-4[4′(-X)-styryl pyridinium iodides/hydrochloric acid systems. *Materials Chemistry and Physics* **110**,145-154 (2008).

54. Issaadi S., Douadi T., Zouaoui A., Chafaa S., Khan M.A., Bouet G., Novel thiophene symmetrical Schiff base compounds as corrosion inhibitor for mild steel in acidic media. *Corrosion Science* **53**,1484-1488 (2011).

55. Behpour M., Ghoreishi S., Soltani N., Salavati-Niasari M., The inhibitive effect of some bis-N, S-bidentate Schiff bases on corrosion behaviour of 304 stainless steel in hydrochloric acid solution. *Corrosion Science* **51**,1073-1082 (2009).

56. Mistry B.M., Kim D.H., Jauhari S., Analysis of Adsorption Properties and Corrosion Inhibition of Mild Steel in Hydrochloric Acid Solution by Synthesized Quinoline Schiff Base Derivatives. *Transactions of the Indian Institute of Metals*:1-13 (2016).

57. Chaieb E., Bouyanzer A., Hammouti B., Benkaddour M., Inhibition of the corrosion of steel in 1 M HCl by eugenol derivatives. *Applied Surface Science* **246**,199-206 (2005).

58. Kliškić M., Radošević J., Gudić S., Katalinić V., Aqueous extract of Rosmarinus officinalis L. as inhibitor of Al–Mg alloy corrosion in chloride solution. *Journal of Applied Electrochemistry* **30**, 823-830 (2000).

59. Singh P., Quraishi M., Corrosion inhibition of mild steel using Novel Bis Schiff's Bases as corrosion inhibitor: Electrochemical and Surface measurement. Measurement **86**,114-124 (2016).

استخدام ن-أمين فيثاليميد كمحضر لأملاح الشيف غير متجانسة الحلقة: لاستخدمها بفاعلية كمثبط لتآكل الصلب منخفض الكربون في محلول٥,٠ مولار من سلفوريك أسيد.

محمد محمود عبد العال`١`، سعد جمعه محمد`١`، يسري فتح الله بركات`١`، حامد يونس دربالة`٢`، حمدي حسنين حسن`٢` و وائل الزعبيج`٣`

`١`معهد التبين للدراسات المعدنية ـ حلوان، القاهرة ص.ب. ١١٤٢١

`٢`قسم الكيمياء ـ كلية العلوم ـ جامعة عين شمس ـ العباسية ـ القاهرة.

`٣`كلية علوم المواد والهندسة ـ جامعة يونجنام ـ جيونجسانج ـ كوريا الجنوبية.

حُضرت عدة أملاح شيف لتثبيط معدل تفاعلات تآكل الصلب منخفض الكربون في الوسط الحمضي، وأثبت التركيب الكيميائي لها باستخدام عدة تقنيات، كما استخدم نموذج لانجمير الايزوثرمي لحساب معاملات الامتزاز. تبين أن وجود أيونات اليوديد في الوسط الحمضي يساعد على زيادة كفاءة أملاح الشيف كعامل مثبط. استخدمت تقنية المعاوقة الكهربية لحساب مقاومة التآكل كما استخدم الميكروسكوب الإلكتروني لاكتشاف شكل سطح الصلب قبل وبعد استخدام مثبطات التآكل. أظهرت النتائج أن المثبطات ذات الشكل المستوي أكثر كفاءة من غيرها الغنية بالإلكترونات لأنها تغطي مساحة أوسع. كما أوضحت النتائج أن ميكانيكية عمل هذه المثبطات تعتمد على تقليل التيار الكاثودي والأنودي.